



Two-fold addition reaction of silylene to C₆₀: structural and electronic properties of a bis-adduct

Masahiro Kako^{*1}, Masato Kai¹, Masanori Yasui¹, Michio Yamada², Yutaka Maeda² and Takeshi Akasaka³

Full Research Paper

Open Access

Address:

¹Department of Engineering Science, The University of Electro-Communications, Chofu 182-8585, Japan, ²Department of Chemistry, Tokyo Gakugei University, Tokyo 184-8501, Japan and ³TARA Center, University of Tsukuba, Tsukuba 305-8577, Japan

Email:

Masahiro Kako^{*} - m.kako@uec.ac.jp

^{*} Corresponding author

Keywords:

bis-adduct; C₆₀; fullerene; silirane; silylene

Beilstein J. Org. Chem. **2024**, *20*, 1179–1188.

<https://doi.org/10.3762/bjoc.20.100>

Received: 01 December 2023

Accepted: 30 April 2024

Published: 22 May 2024

This article is part of the thematic issue "Carbon-rich materials: from polyaromatic molecules to fullerenes and other carbon allotropes".

Guest Editor: Y. Yamakoshi



© 2024 Kako et al.; licensee Beilstein-Institut.
License and terms: see end of document.

Abstract

The addition reaction of C₆₀ with silylene **1**, a silicon analog of carbene, yielded the corresponding bis-adduct **3**. The structure of **3** was determined by single-crystal X-ray structure analysis, representing the first example of a crystal structure of a silirane (silacyclopropane) derivative of fullerenes. Electrochemical measurements confirmed that the redox potentials of **3** are shifted cathodically compared to those of the parent mono-adduct **2**. Density functional theory (DFT) calculations provided the basis for the electronic properties of compound **3**.

Introduction

The chemical functionalization of fullerenes has been exploited extensively from both fundamental and practical perspectives, elucidating their potential applications for biochemistry, nanomaterials sciences, and molecular electronics [1-3]. With the development of research investigating the functionalization of fullerenes, several multiple addition reactions of fullerenes have been investigated [4-8]. For example, earlier reports have described that some functionalization reactions of fullerenes afford bis-adducts with excellent properties as organic photovoltaic materials [9-14]. Furthermore, regioisomerically pure bis-functionalized fullerenes function better as electron accep-

tors in organic thin-film solar cells than mixtures of the corresponding regioisomers do [12-14]. Therefore, controlling the regioselectivities of multiple functionalizations of fullerenes for the selective synthesis of specific multi-adducts poses an important challenge.

Addition reactions of C₆₀ are well known to occur mainly at the 6,6-bonds (junction between two hexagons) rather than at the 5,6-bonds (junction between a pentagon and a hexagon). If the second additions proceed also at the 6,6-bonds, then nine regioisomers are possible for bis-additions, as shown in Figure 1

[4,5]. In addition, when the second addends are identical to the first, the e' and e'' isomers are the same adducts, thereby affording eight possible regioisomers for bis-addition reactions. Hirsch and co-workers reported two-fold additions of C_{60} using the Bingel–Hirsch and the Bamford–Stevens reactions as well as nitrene addition reactions, indicating the formation of regioisomers as anticipated from the possible addition sites in Figure 1 [5]. Diederich and co-workers developed a general methodology using tether-directed remote functionalization for the regioselective formation of multiple adducts of fullerenes [6].

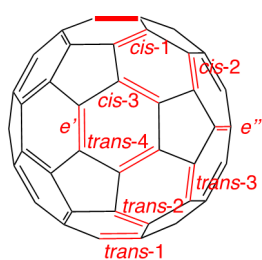


Figure 1: Positional notation of 6,6-bonds in a mono-adduct of C_{60} with the first addition site indicated using a bold line [5].

In our earlier reports, the reactions of C_{60} and C_{70} , with silylene Dip_2Si (**1**, $Dip = 2,6$ -diisopropylphenyl), a silicon analog of carbene, were described as providing silirane (silacyclopropane)-type 6,6-mono-adducts Dip_2SiC_{60} (**2**, Scheme 1) and Dip_2SiC_{70} [15,16]. Furthermore, bis-adducts $(Dip_2Si)_2C_{60}$ and $(Dip_2Si)_2C_{70}$ were obtained as byproducts, but no details of these bis-adducts have been clarified [15,16]. The results demonstrated that the electronic properties of product **2** were altered considerably compared to that of pristine C_{60} mainly because silicon atoms are less electronegative. Electron-donating effects of silyl groups in fullerene derivatives were also

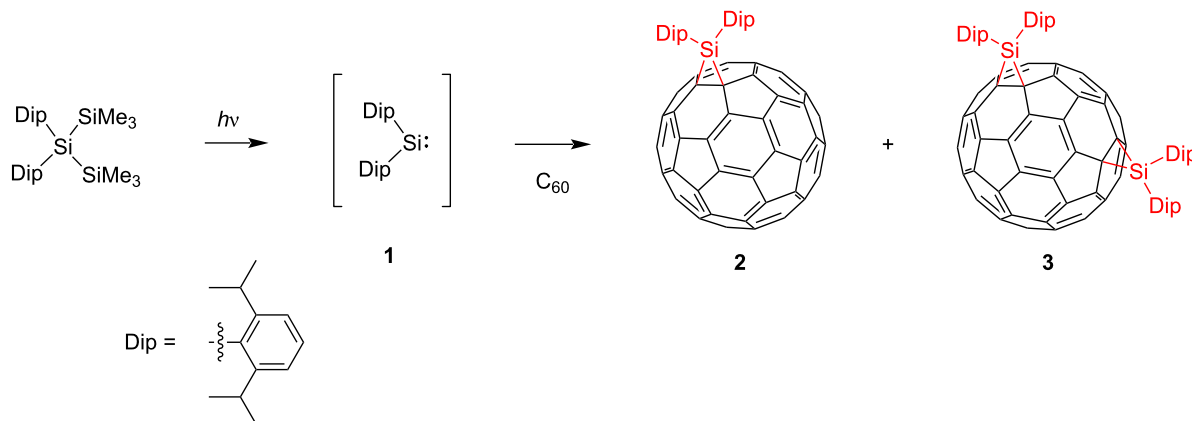
rationalized in terms of σ – π conjugations between C–Si σ bonds of the silirane ring and adjacent π -bonds of the fullerene cage [17–20]. Therefore, it is interesting to examine the electronic properties of multi-silylene adducts in comparison with those of **2**. Herein, we report the structural determination and characterization of a bis-silylene adduct **3** of C_{60} based on spectroscopic measurements, X-ray crystallography, electrochemical analyses, and theoretical calculations.

Results and Discussion

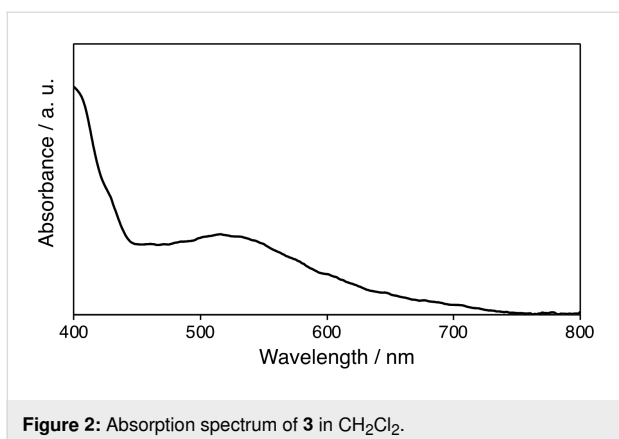
Synthesis of bis-silylene adduct **3**

The synthesis of the silylene adduct was conducted using a modified literature procedure [15]. A degassed solution of $Dip_2Si(SiMe_3)$ as a silylene precursor and C_{60} in toluene was irradiated by a 125-W low-pressure mercury lamp in a quartz tube for 2 h (Scheme 1). During reaction, the color of the solution turned to dark brown. After the photolysis, the bis-silylene adduct **3** was isolated in 36% yield accompanied by mono-adduct **2** (22% yield) by silica gel flash column chromatography using mixed solvents of hexane/ CH_2Cl_2 by changing the ratios of volumes from 10:1 to 3:1. In thin-layer chromatography (TLC) analysis using silica gel, the R_f values are 0.55 for **2** and 0.33 for **3**, respectively, with hexane/ CH_2Cl_2 5:1 as solvent mixture. Although several other fractions containing C_{60} derivatives were obtained, their structures are still under investigation because of the difficulty in isolating and purifying those fractions.

To clarify the addition site of **3**, we measured the ultraviolet–visible (UV–vis) spectrum. Fullerene derivatives are well-known to show characteristic absorption spectra depending on the addition pattern. As shown in Figure 2, the spectrum of **3** exhibited an absorption maximum at 515 nm, which is similar to those of the e' and e'' isomers of $C_{60}[C(C_6H_4OMe)_2]_2$ and $C_{60}[C(C_6H_4OMe)_2][NCOOEt]$ [5]. In the case of **3**, the e' and

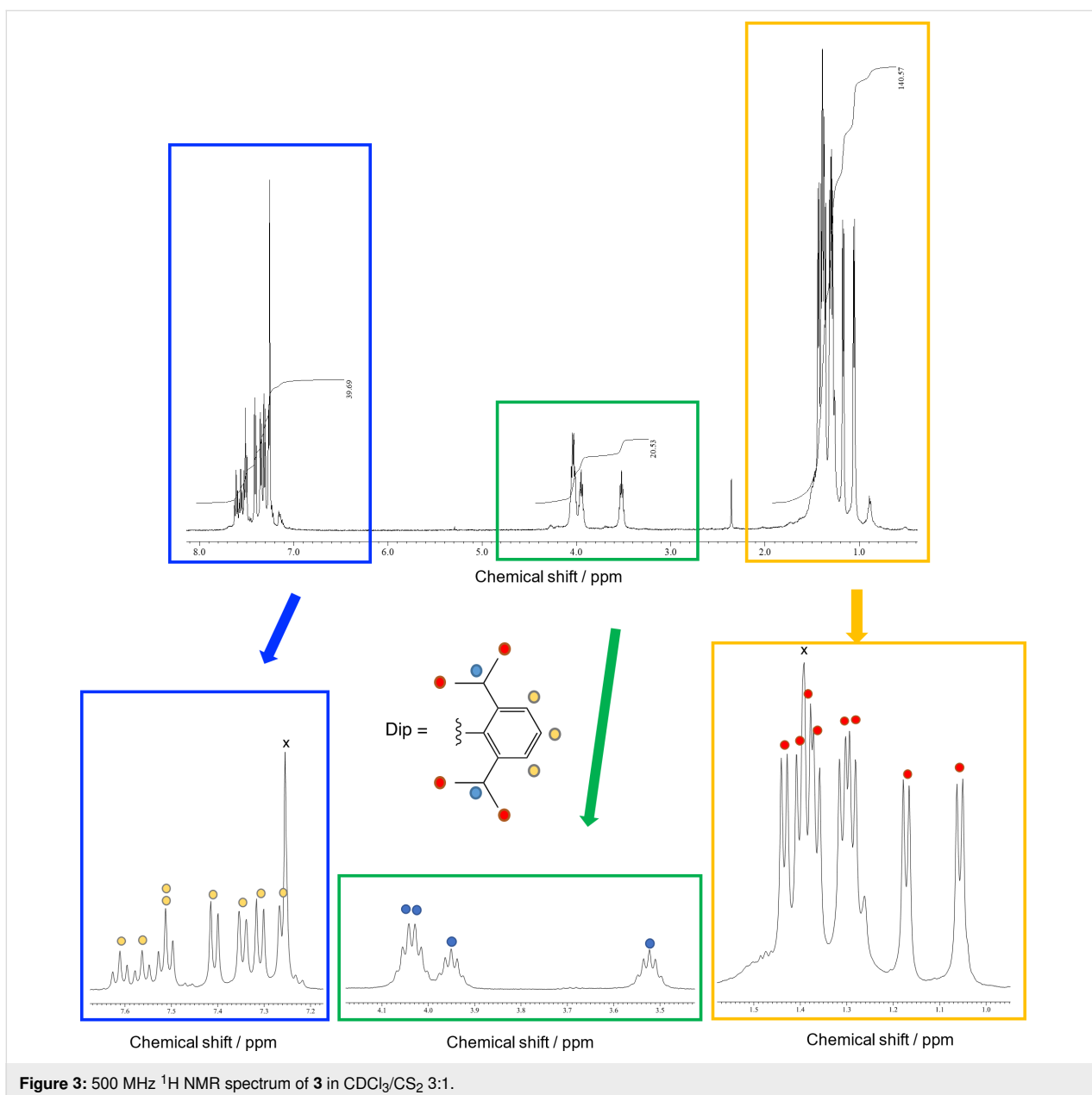


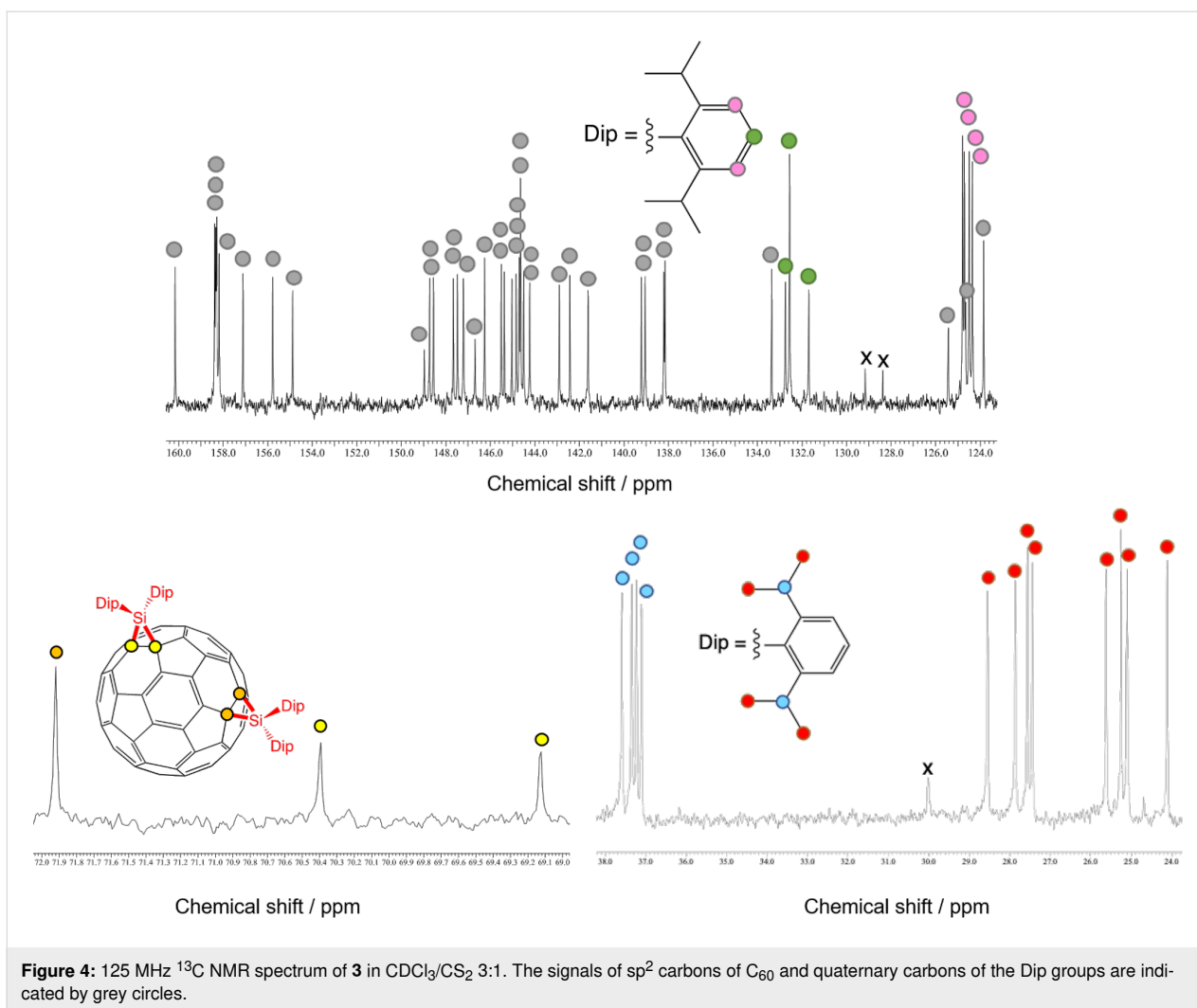
Scheme 1: Synthesis of silylene adducts **2** and **3**.



e'' isomers are identical products, and **3** is denoted as the *e* isomer hereinafter.

The ¹H NMR spectrum of **3** showed signals of eight doublets and three septets, which were assigned respectively to the methyl and methine groups, along with the aromatic protons (Figure 3). In the ¹³C NMR spectrum, a total of 43 signals were observed in the low-field region (approximately 160–120 ppm), of which 29 signals are attributed to the C₆₀ carbon cage and 14 signals are attributed to the aromatic ring carbon nuclei of the Dip groups (Figure 4). In addition, three sp³ carbon atoms of the C₆₀ carbon cage, eight methyl, and three methine carbon signals of the Dip group were observed. These spectral features





are consistent with the structure of **3** as the *e* isomer of bis-adducts with C_s symmetry. The plane of symmetry includes one silirane ring and bisects another silirane ring perpendicularly.

Unfortunately, the matrix-assisted laser desorption ionization time-of-flight (MALDI-TOF) mass spectrometry of **3** afforded no molecular ion peak expected for adducts derived from Dip_2Si and C_{60} while a base peak at m/z 720 due to C_{60} was observed probably because of the low stability of radical ions of **3**.

Finally, the structure of **3** was established by single-crystal X-ray structure analysis. The ORTEP diagram of **3** is presented in Figure 5 with the selected bond lengths and angles collected in Table 1. The cage C–C bond lengths of the addition sites are C1–C9: 1.623(2) Å and C21–C40: 1.6282(19) Å, which fall within the range of the corresponding values reported for the crystal structures of methano-derivatives of C_{60} [5,21–33]. It is noteworthy that these C–C bond lengths are longer than those of

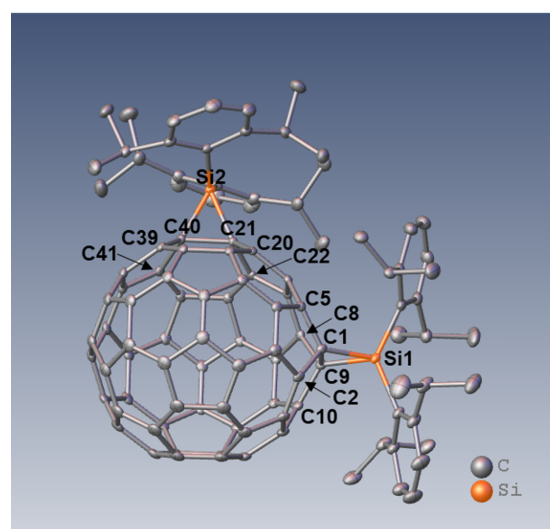


Figure 5: ORTEP drawing of **3** showing thermal ellipsoids at the 50% probability level at 100 K. Hydrogen atoms are omitted for clarity.

Table 1: Selected bond lengths and angles of **3**.

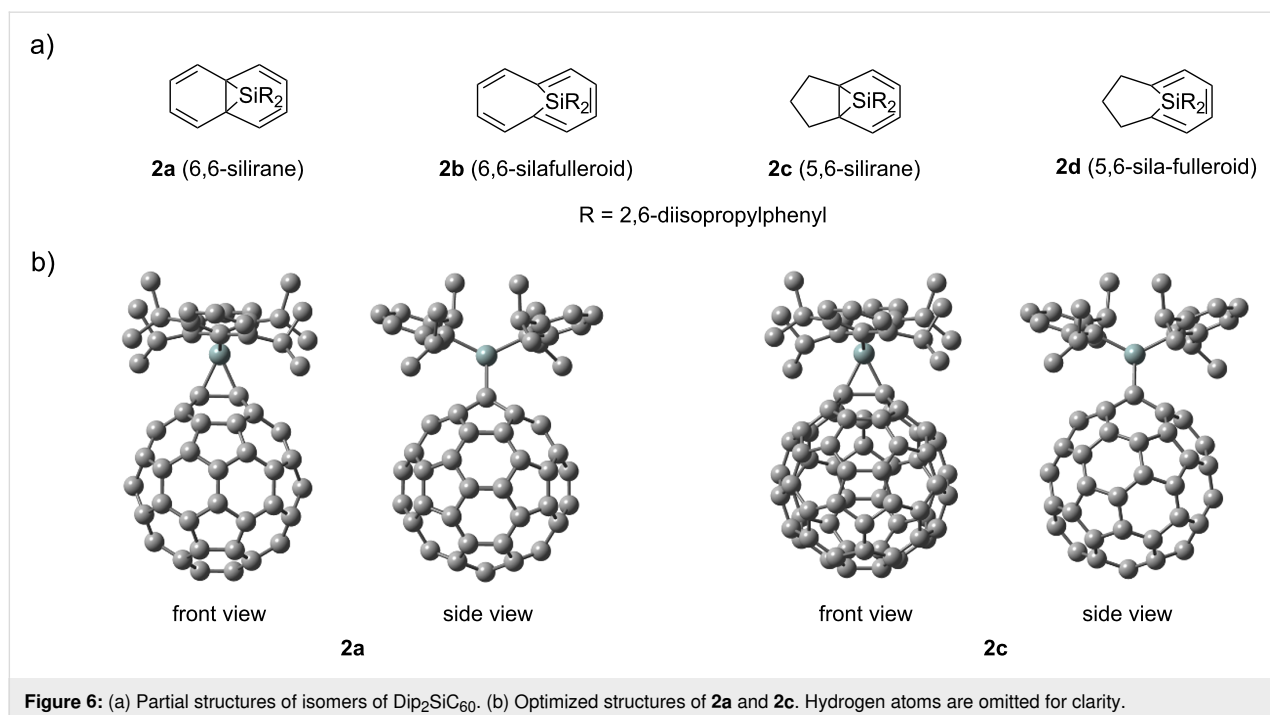
bond length [Å]		bond angle [°]	
C1–C9	1.623(2)	Si1–C1–C9	64.19(7)
Si1–C1	1.8886(15)	C1–Si1–C9	51.04(6)
Si1–C9	1.8796(15)	Si1–C9–C1	64.77(7)
C1–C2	1.495(2)		
C1–C5	1.497(2)		
C8–C9	1.492(2)		
C9–C10	1.498(2)		
C21–C40	1.6282(19)	Si2–C21–C40	64.65(7)
Si2–C21	1.8778(14)	C21–Si2–C40	51.26(6)
Si2–C40	1.8865(15)	Si2–C40–C21	64.10(7)
C20–C21	1.4951(19)		
C21–C22	1.490(2)		
C39–C40	1.4951(19)		
C40–C41	1.4928(19)		

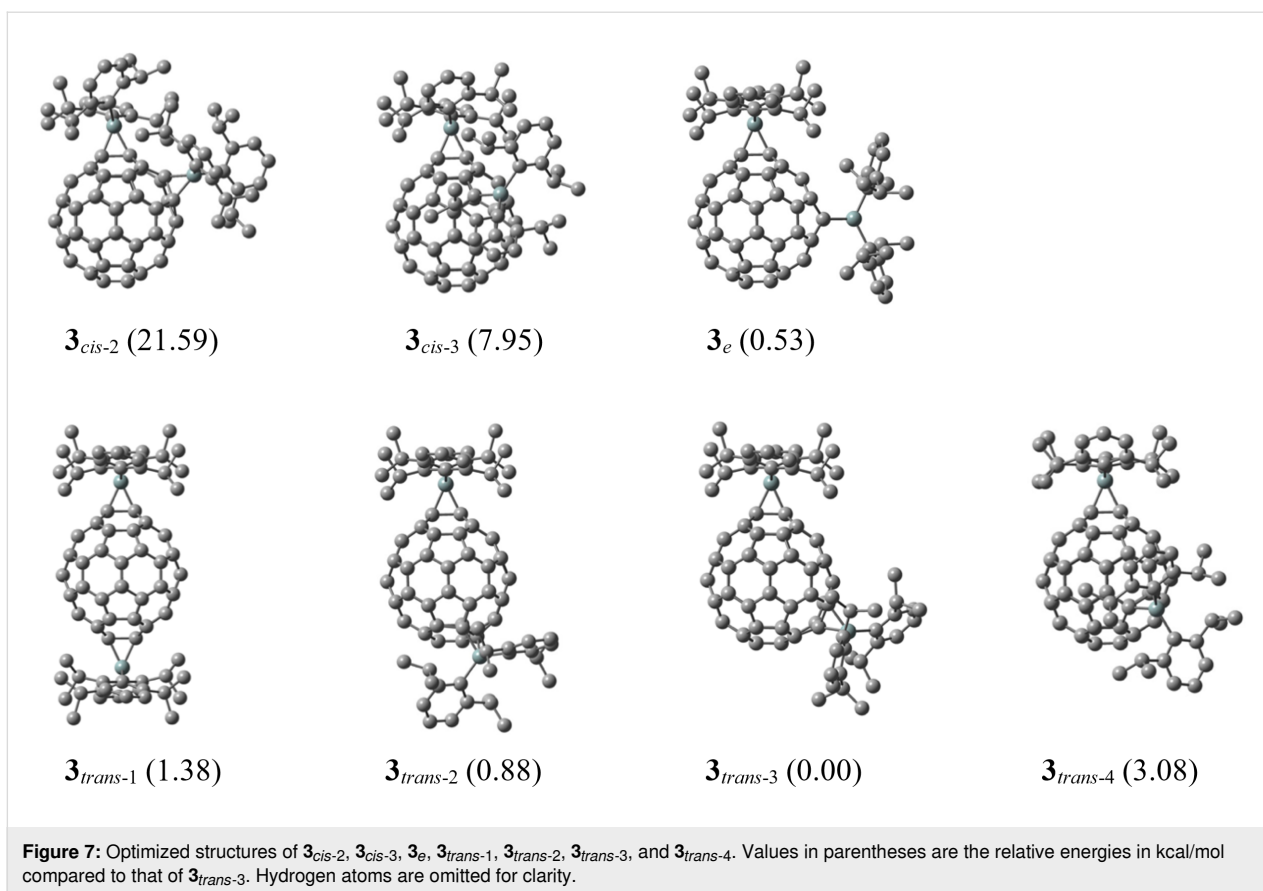
the reported siliranes [34–42], except for rare examples such as 3-(hydroxydimesitylsilyl)-1,1-dimesityl-2,2-bis(trimethylsilyl)-1-silirane [43]. In contrast, we earlier reported the crystal structure of the adduct of $\text{Lu}_3\text{N}@I_h\text{-C}_{80}$ with silylene Dep_2Si ($\text{Dep} = 2,6\text{-diethylphenyl}$), which was revealed to be a sila-fulleroid structure with the cage C–C separation distance of 2.25 Å at the addition site [44]. On the other hand, the Si–C bond lengths of the silirane ring in **3** are Si1–C1: 1.8886(15) Å, Si1–C9: 1.8796(15) Å, Si2–C21: 1.8778(14) Å, and Si2–C40: 1.8865(15) Å, which are roughly equal to those of the reported

siliranes. These results confirm that the two addends in **3** are both silirane structures, which represents the first example of a crystallographic analysis of silirane derivatives of fullerenes.

Theoretical calculations

Hirsch and co-workers reported the bis-functionalization of C_{60} using the Bingel–Hirsch, the Bamford–Stevens reactions, and nitrene addition, indicating that preferential formation of the *e* (*e'* or *e''*) isomers followed by *trans*-3 isomer when at least one of the two addends was sterically demanding [5]. The formation of **3** in the present bis-silylene addition is consistent with those earlier results. To obtain some insight into regioselectivity, we performed density functional theory (DFT) calculations using the B3LYP/6-31G(d) method [45–48]. We first compared the relative stabilities of mono-adducts ($\text{Dip}_2\text{SiC}_{60}$) with 6,6-silirane (**2a**), 6,6-sila-fulleroid (**2b**), 5,6-silirane (**2c**), and 5,6-sila-fulleroid (**2d**) structures (Figure 6). The optimized structure of **2a** was found to be more stable than that of **2c** by 19.23 kcal/mol. In contrast, optimization using initial structures of **2b** and **2d** afforded the structures of **2a** and **2c**, respectively. Based on these results, the optimized structures of bis-adduct isomers **3**_{*cis*-2}, **3**_{*cis*-3}, **3**_{*e*}, **3**_{*trans*-1}, **3**_{*trans*-2}, **3**_{*trans*-3}, and **3**_{*trans*-4} were calculated by assuming the 6,6-silirane structures for addition sites. Calculation of **3**_{*cis*-1} was not conducted because of its sterically clouded structure. Structural parameters around the addition sites of **3**_{*e*} showed rough agreement with the corresponding values of **3** obtained using the X-ray structural analysis (Table 1 and Table S1 in Supporting Information File 1). As shown in Figure 7, few differences in relative energies are

**Figure 6:** (a) Partial structures of isomers of $\text{Dip}_2\text{SiC}_{60}$. (b) Optimized structures of **2a** and **2c**. Hydrogen atoms are omitted for clarity.



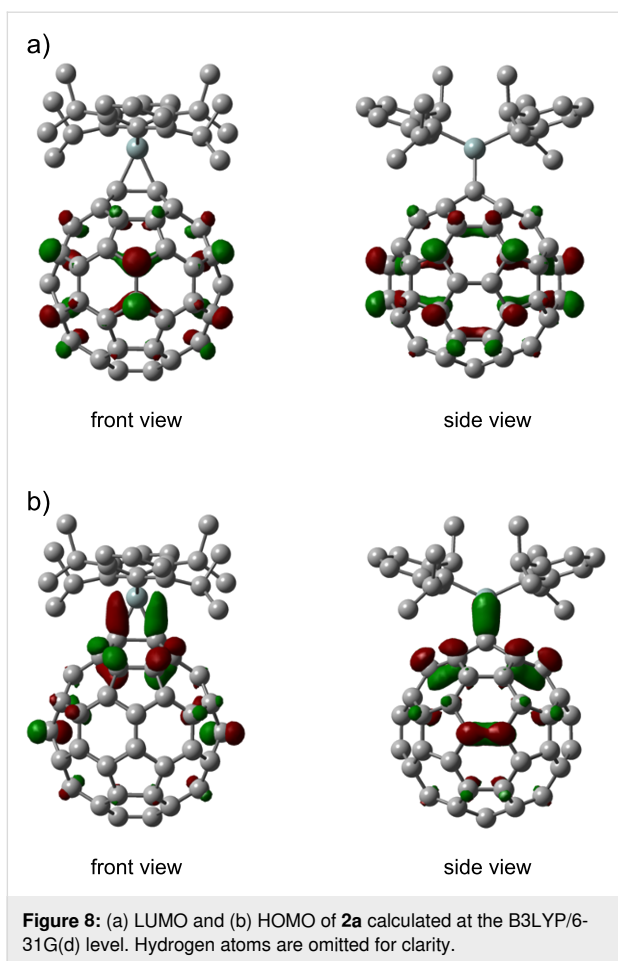
apparent among $\mathbf{3}_e$, $\mathbf{3}_{trans-1}$, $\mathbf{3}_{trans-2}$, $\mathbf{3}_{trans-3}$, and $\mathbf{3}_{trans-4}$, although $\mathbf{3}_{cis-2}$ and $\mathbf{3}_{cis-3}$ are unstable. Therefore, we next investigated the structural and electronic properties of the calculated mono-adduct $\mathbf{2a}$ to evaluate its reactivity toward $\mathbf{1}$.

The bond lengths of the cage C–C double bonds and the π -orbital axis vector (POAV) [49] of the cage carbon atoms of $\mathbf{2a}$ are presented in Tables S2 and S3 in Supporting Information File 1. Mean values are given respectively for the identical type of bonds and atoms. The differences in the double bond lengths are negligible, but the *cis*-1, *cis*-2, and *e* bonds are slightly shorter than the other bonds. The POAV values show no marked difference except for the carbons adjacent to the addition site. Therefore, neither the double bond lengths nor the POAV values of $\mathbf{2a}$ are regarded as affecting the regioselectivity.

The frontier orbitals of $\mathbf{2a}$ were then examined to elucidate the reactivity in the second silylene addition. The ground states of silylenes are known to be singlet except for a few examples [50,51]. Singlet silylenes have *n* orbitals as the highest occupied molecular orbitals (HOMOs) that accommodate unshared electron pairs on the silicon atoms, while empty 3*p* orbitals correspond to the lowest unoccupied molecular orbitals (LUMOs).

In addition, silylenes are characterized by both nucleophilic properties based on the high HOMO levels, and electrophilic properties because of the low LUMO levels [50,51]. The Mulliken charge densities of $\mathbf{2s}$ are also shown in Figure S2 (Supporting Information File 1), which shows that the charge densities are nearly zero on the cage carbon atoms except those adjacent to the addition site. The charge densities of $\mathbf{2a}$ are regarded as affecting the regioselectivity. Thus, it is suggested that the regioselectivity in the silylene addition could not be estimated by the charge densities of $\mathbf{2a}$.

The regioselectivity in the addition reaction of $\mathbf{1}$ with C_{70} was explained earlier in terms of the interaction between the HOMO of $\mathbf{1}$ and the LUMO of C_{70} [16]. The reaction mechanism of ethylene with a silylene substituted with thiolate ligands has been studied using theoretical calculations, in which the transition state was ascribed to the donor–acceptor interactions between the HOMO of the silylene and the LUMO of ethylene, and vice versa [42]. For $\mathbf{2a}$, the LUMO is largely distributed at the *e'* bonds, followed by the *cis*-2 and *trans*-3 bonds (Figure 8). These results suggest that the formation of $\mathbf{3}$ may involve the interaction of $\mathbf{1}$ with the LUMO of $\mathbf{2a}$. The HOMO of $\mathbf{2a}$ is observed mainly around the *cis*-1 and *e''* bonds among the 6,6-bonds, although the *cis*-1 bond would not be susceptible to the



second silylene addition because of its steric hindrance. Alternatively, the interaction of the LUMO of **1** with the HOMO of **2a** should be considered.

Electrochemical measurements of **3**

Cyclic voltammetry (CV) and differential pulse voltammetry (DPV) measurements were conducted to evaluate the electronic effects of the silylene addends in **3** (Figure 9). The oxidation processes of **3** were shown to be irreversible, probably because of the removal of silylene addends, whereas the electrochemically reversible behavior was observed for the reduction waves. Table 2 presents the redox potentials of **3** obtained by DPV with those of C₆₀ and **2**, as reference compounds. Both the reduction (E^{red}) and the oxidation (E^{ox}) potentials of **3** were found to be shifted cathodically compared respectively to those of C₆₀ and **2**, indicating the electron-donating effects of the two Dip₂Si groups. It is noteworthy that the first reduction potential of **3** ($E^{\text{red}}_1 = -1.52$ V) is the most negative among those of the silylated empty fullerenes [52-56].

The energies of HOMOs and LUMOs of the calculated regioisomers of **3** were compared with those of C₆₀ and **2a** (Table 3).

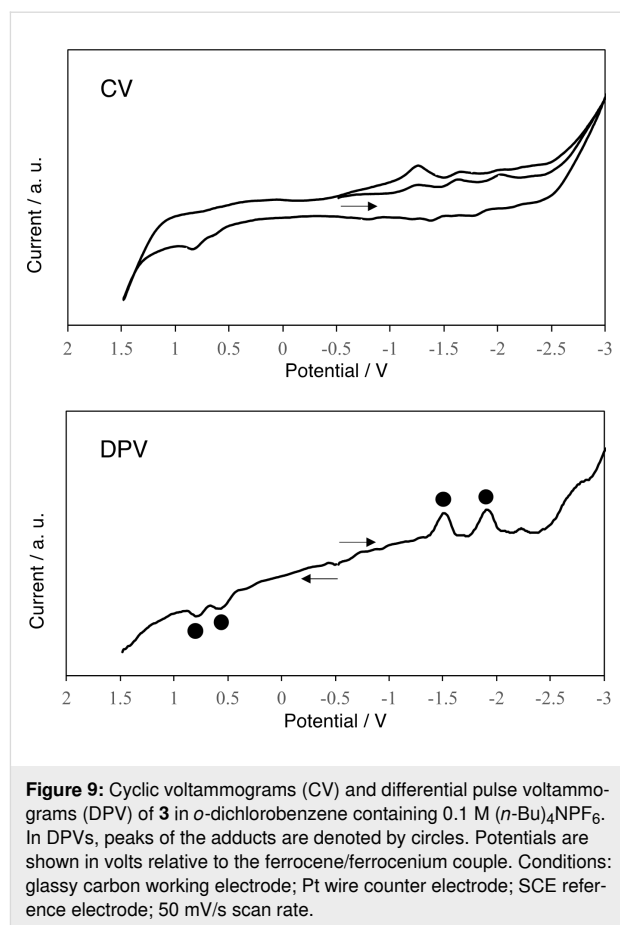


Table 2: Redox potentials^a (V) of C₆₀, **2**, and **3**.

compound	E^{ox}_2	E^{ox}_1	E^{red}_1	E^{red}_2
C ₆₀		+1.32 ^b	-1.15	-1.58
2 ^b		+0.71	-1.30	-1.71
3	+0.80	+0.58	-1.52	-1.92

^aValues obtained by DPV are in volts relative to the ferrocene/ferrocenium couple. ^bData from ref [54].

The HOMO and LUMO levels of **3_e** were both found to be higher than those of C₆₀ and **2a**, respectively, which is qualitatively consistent with the shifts in the redox potentials of C₆₀, **2**, and **3**. By contrast, **3_{cis-2}**, **3_{cis-3}**, **3_e**, **3_{trans-1}**, **3_{trans-2}**, **3_{trans-3}**, and **3_{trans-4}** were found to have no significant differences in their respective HOMO and LUMO levels, as shown in Table 3.

Conclusion

The bis-silylene adduct **3** was isolated by the two-fold addition of **1** to C₆₀. The spectroscopic and crystallographic analyses established **3** as an *e* isomer of bis-adducts with silirane structures at the 6,6-bonds. In the DFT calculations of mono-adduct **2a**, the LUMO is distributed remarkably around the *e'* bonds,

Table 3: Calculated HOMO/LUMO levels (eV)^a.

compound	HOMO	LUMO
C ₆₀	−5.99	−3.23
2a	−5.30	−2.91
3 _{cis-2}	−5.14	−2.68
3 _{cis-3}	−4.77	−2.62
3 _e	−5.01	−2.61
3 _{trans-1}	−4.99	−2.67
3 _{trans-2}	−4.97	−2.67
3 _{trans-3}	−4.90	−2.58
3 _{trans-4}	−4.86	−2.58

^aB3LYP/6-31G(d).

which are likely to interact with the HOMO of **1** leading to the formation of **3**. Also, the HOMO of **2a** is observed around the *cis*-1 and *e''* bonds, although the *cis*-1 bond would be sterically protected from the second silylene addition. Alternatively, the interaction of the LUMO of **1** with *e''* bonds of **2** should be considered. Electrochemical measurements (CV and DPV) were taken to evaluate the electronic properties of **3**. As expected, the redox potentials of **3** are shown to be shifted cathodically compared to those of C₆₀ and **2** because of the electron-donating effect of the two silylene groups. These results are qualitatively consistent with the shifts in the HOMO and LUMO levels calculated respectively for C₆₀, **2**, and **3**.

Experimental

Materials and general method: All chemicals were reagent grade, purchased from commercial suppliers. *o*-Dichlorobenzene (ODCB) was distilled from P₂O₅ under vacuum before use. Toluene was distilled from benzophenone sodium ketyl under dry N₂ prior to use. Reagents were used as purchased unless otherwise specified. The ¹H and ¹³C NMR measurements were conducted on a JEOL ECA-500 spectrometer (JEOL Ltd.). Absorption spectra were measured using a UV-3150 spectrophotometer (Shimadzu Corp.). Cyclic voltammograms and differential pulse voltammograms were recorded on a BAS CV50W electrochemical analyzer (BAS Inc.). The reference electrode was a saturated calomel reference electrode (SCE). The glassy carbon electrode was used as the working electrode, and a platinum wire was used as the counter electrode. All potentials are referenced to the ferrocene/ferrocenium couple (Fc/Fc⁺) as the standard. (*n*-Bu)₄NPF₆ (0.1 M) in ODCB was used as the supporting electrolyte solution. The cyclic voltammograms were recorded using a scan rate of 50 mV/s. The differential pulse voltammograms were obtained using a pulse amplitude of 50 mV, a pulse width of 50 ms, a pulse period of 200 ms, and a scan rate of 50 mV/s.

Synthesis of 3. A degassed solution of Dip₂Si(SiMe₃) (30 mg) and C₆₀ (4.6 mg) in toluene (20 mL) in a quartz tube was irradiated by a 125-W low-pressure mercury lamp for 2 h [15]. After the photolysis, **2** (22% yield) and **3** (36% yield) were isolated by flash column chromatography (SiO₂) using mixed solvents of hexane/CH₂Cl₂ by changing the ratios of volumes from 10:1 to 3:1. TLC analysis (SiO₂, hexane/CH₂Cl₂ 5:1) afforded R_f = 0.55 for **2** and R_f = 0.33 for **3**, respectively. Data for compound **3**: ¹H NMR (CDCl₃/CS₂ 3:1) δ 7.61 (t, *J* = 7.5 Hz, 1H), 7.56 (t, *J* = 7.5 Hz, 1H), 7.51 (t, *J* = 7.5 Hz, 2H), 7.41 (d, *J* = 7.5 Hz, 2H), 7.35 (d, *J* = 7.5 Hz, 2H), 7.31 (d, *J* = 7.5 Hz, 2H), 7.26 (d, *J* = 7.5 Hz, 2H), 4.04 (sept, *J* = 7.0 Hz, 2H), 4.03 (sept, *J* = 7.0 Hz, 2H), 3.95 (sept, *J* = 7.0 Hz, 2H), 3.52 (sept, *J* = 7.0 Hz, 2H), 1.43 (d, *J* = 7.0 Hz, 6H), 1.40 (d, *J* = 7.0 Hz, 6H), 1.371 (d, *J* = 7.0 Hz, 6H), 1.365 (d, *J* = 7.0 Hz, 6H), 1.31 (d, *J* = 7.0 Hz, 6H), 1.29 (d, *J* = 7.0 Hz, 6H), 1.17 (d, *J* = 7.0 Hz, 6H), 1.06 (d, *J* = 7.0 Hz, 6H); ¹³C NMR (CDCl₃/CS₂ 3:1) δ 160.16 (s, 2C), 158.38 (s, 2C), 158.33 (s, 2C), 158.29 (s, 2C), 158.18 (s, 2C), 157.12 (s, 2C), 155.78 (s, 2C), 154.87 (s, 2C), 148.96 (s, 1C), 148.73 (s, 2C), 148.56 (s, 2C), 147.66 (s, 2C), 147.48 (s, 2C), 147.22 (s, 2C), 146.69 (s, 1C), 146.26 (s, 2C), 145.51 (s, 2C), 145.37 (s, 2C), 145.03 (s, 2C), 144.84 (s, 2C), 144.71 (s, 2C), 144.65 (s, 4C), 144.51 (s, 2C), 144.23 (s, 2C), 142.90 (s, 2C), 142.43 (s, 2C), 141.62 (s, 2C), 139.22 (s, 2C), 139.05 (s, 2C), 138.21 (s, 2C), 138.15 (s, 2C), 133.37 (s, 2C), 132.76 (d, 1C), 132.56 (d, 2C), 131.71 (d, 1C), 125.43 (s, 1C), 124.79 (d, 2C), 124.71 (d, 2C), 124.66 (s, 1C), 124.49 (d, 2C), 124.35 (d, 2C), 123.85 (s, 2C), 71.92 (s, 2C), 70.39 (s, 1C), 69.12 (s, 1C), 37.59 (d, 2C), 37.35 (d, 2C), 37.24 (d, 2C), 37.11 (d, 2C), 28.55 (q, 2C), 27.86 (q, 2C), 27.57 (q, 2C), 27.44 (q, 2C), 25.61 (q, 2C), 25.25 (q, 2C), 25.10 (q, 2C), 24.11 (q, 2C); UV-vis (CH₂Cl₂) λ_{max} 515 nm.

X-ray crystallography of 3: Black plate crystals suitable for X-ray diffraction were obtained using the liquid–liquid bilayer diffusion method with solutions of **3** in CS₂ using hexane as a poor solvent at 0 °C. Single-crystal X-ray diffraction data of **3** were collected on a Rigaku Oxford Diffraction XtaLAB Synergy R DW system with a HyPix detector equipped with a nitrogen-gas flow low-temperature apparatus providing a constant temperature at 100 K. Crystal data for C₆₀(Dip₂Si)₂: C₁₀₈H₆₈Si₂; *M*_r = 1421.87, black plate, 0.11 × 0.16 × 0.025 mm, λ = 0.71073 Å, monoclinic, space group *P*2₁/*n* (no. 14), *a* = 18.3631(3), *b* = 13.6696 (2), *c* = 27.6360 (5) Å, β = 92.857 (2)°, *V* = 6928.5(2) Å³, *T* = 99.9(2) K, *Z* = 4, 67750 reflections measured, 19176 unique (*R*_{int} = 0.0321), which were used for all calculations, 2θ_{max} = 63.262; min/max transmission = 0.921/1.000 (absorption correction was applied by multi-scan method); The structure was solved using a direct method using olex2.solve 1.5-ac5-018 [57] and was refined with SHELXL-2018 [58]. The final *wR*(F₂) was 0.1283 (all data),

conventional $R_1 = 0.0493$ computed for 14459 reflections with $I > 2\sigma(I)$ using 1007 parameters with 0 restraints. Crystallographic computations were performed with Olex2 [59]. CCDC 2311474 (3) contains the supplementary crystallographic data for this paper, and is obtainable free of charge from the Cambridge Crystallographic Data Centre.

Computational method. All calculations were conducted using the Gaussian 16 program [60]. Optimized structures were obtained at the B3LYP [45–47] level of theory using basis sets of 6-31G(d) [48].

Supporting Information

Supporting Information File 1

Structural data of **2a** and **3e** obtained by DFT calculations, and Cartesian coordinates of optimized structures.
[<https://www.beilstein-journals.org/bjoc/content/supplementary/1860-5397-20-100-S1.pdf>]

Supporting Information File 2

Crystallographic information file of **3**.
[<https://www.beilstein-journals.org/bjoc/content/supplementary/1860-5397-20-100-S2.cif>]

Funding

This work was supported by Grants-in-Aid for Scientific Research (B) (No. 24350019) and (C) (No. 17K05797 and 20K05469) from the Ministry of Education, Culture, Sports, Science, and Technology of Japan.

Author Contributions

Masahiro Kako: conceptualization; supervision; writing – original draft; writing – review & editing. Masato Kai: investigation. Masanori Yasui: investigation. Michio Yamada: investigation; writing – review & editing. Yutaka Maeda: investigation; writing – review & editing. Takeshi Akasaka: conceptualization; writing – review & editing.

ORCID® iDs

Masahiro Kako - <https://orcid.org/0000-0002-2669-5870>
Masanori Yasui - <https://orcid.org/0009-0006-3157-9862>
Michio Yamada - <https://orcid.org/0000-0002-6715-4202>
Yutaka Maeda - <https://orcid.org/0000-0003-0502-5621>
Takeshi Akasaka - <https://orcid.org/0000-0002-4073-4354>

Data Availability Statement

All data that supports the findings of this study is available in the published article and/or the supporting information to this article.

References

- Hirsch, A. *The Chemistry of the Fullerenes*; Thieme: Stuttgart, Germany, 1994. doi:10.1002/9783527619214
- Taylor, R., Ed. *The Chemistry of the Fullerenes; Advanced Series in Fullerenes*, Vol. 4; World Scientific: Singapore, 1995. doi:10.1142/2790
- Hirsch, A., Ed. *Fullerenes and related Structures*; Springer: Berlin, Germany, 1999. doi:10.1007/3-540-68117-5
- Hirsch, A.; Lamparth, I.; Karfunkel, H. R. *Angew. Chem., Int. Ed. Engl.* **1994**, *33*, 437–438. doi:10.1002/anie.199404371
- Djojo, F.; Herzog, A.; Lamparth, I.; Hampel, F.; Hirsch, A. *Chem. – Eur. J.* **1996**, *2*, 1537–1547. doi:10.1002/chem.19960021211
- Diederich, F.; Kessinger, R. *Acc. Chem. Res.* **1999**, *32*, 537–545. doi:10.1021/ar970321o
- Hirsch, A. *Chem. Rec.* **2005**, *5*, 196–208. doi:10.1002/tcr.20047
- Cerón, M. R.; Echegoyen, L. J. *J. Phys. Org. Chem.* **2016**, *29*, 613–619. doi:10.1002/poc.3563
- Brabec, C. J.; Cravino, A.; Meissner, D.; Sariciftci, N. S.; Fromherz, T.; Rispen, M. T.; Sanchez, L.; Hummelen, J. C. *Adv. Funct. Mater.* **2001**, *11*, 374–380. doi:10.1002/1616-3028(200110)11:5<374::aid-adfm374>3.0.co;2-w
- Lenes, M.; Wetzelaer, G.-J. A. H.; Kooistra, F. B.; Veenstra, S. C.; Hummelen, J. C.; Blom, P. W. M. *Adv. Mater. (Weinheim, Ger.)* **2008**, *20*, 2116–2119. doi:10.1002/adma.200702438
- Mishra, A.; Bäuerle, P. *Angew. Chem., Int. Ed.* **2012**, *51*, 2020–2067. doi:10.1002/anie.201102326
- Tao, R.; Umeyama, T.; Kurotobi, K.; Imahori, H. *ACS Appl. Mater. Interfaces* **2014**, *6*, 17313–17322. doi:10.1021/am5058794
- Wong, W. W. H.; Subbiah, J.; White, J. M.; Seyler, H.; Zhang, B.; Jones, D. J.; Holmes, A. B. *Chem. Mater.* **2014**, *26*, 1686–1689. doi:10.1021/cm404054z
- Meng, X.; Zhao, G.; Xu, Q.; Tan, Z.; Zhang, Z.; Jiang, L.; Shu, C.; Wang, C.; Li, Y. *Adv. Funct. Mater.* **2014**, *24*, 158–163. doi:10.1002/adfm.201301411
- Akasaka, T.; Ando, W.; Kobayashi, K.; Nagase, S. *J. Am. Chem. Soc.* **1993**, *115*, 1605–1606. doi:10.1021/ja00057a072
- Akasaka, T.; Mitsuhida, E.; Ando, W.; Kobayashi, K.; Nagase, S. *J. Chem. Soc., Chem. Commun.* **1995**, 1529–1530. doi:10.1039/c39950001529
- Bock, H.; Solouki, B. Photoelectron Spectra of Silicon Compounds. In *The Chemistry of Organic Silicon Compounds*; Patai, S.; Rappoport, Z., Eds.; John Wiley & Sons: Chichester, UK, 1989; pp 555–653. doi:10.1002/0470025107.ch9
- Traylor, T. G.; Hanstein, W.; Berwin, H. J.; Clinton, N. A.; Brown, R. S. *J. Am. Chem. Soc.* **1971**, *93*, 5715–5725. doi:10.1021/ja00751a024
- Hosomi, A. *Acc. Chem. Res.* **1988**, *21*, 200–206. doi:10.1021/ar00149a004
- Fleming, I.; Barbero, A.; Walter, D. *Chem. Rev.* **1997**, *97*, 2063–2192. doi:10.1021/cr941074u
- Osterodt, J.; Nieger, M.; Vögtle, F. *J. Chem. Soc., Chem. Commun.* **1994**, 1607–1608. doi:10.1039/c39940001607
- Anderson, H. L.; Boudon, C.; Diederich, F.; Gisselbrecht, J.-P.; Gross, M.; Seiler, P. *Angew. Chem., Int. Ed. Engl.* **1994**, *33*, 1628–1632. doi:10.1002/anie.199416281
- Paulus, E. F.; Bingel, C. *Acta Crystallogr., Sect. C: Cryst. Struct. Commun.* **1995**, *51*, 143–146. doi:10.1107/s0108270194009728
- Seiler, P.; Isaacs, L.; Diederich, F. *Helv. Chim. Acta* **1996**, *79*, 1047–1058. doi:10.1002/hlca.19960790413

25. Tezuka, Y.; Kawasaki, N.; Yajima, H.; Ishii, T.; Oyama, T.; Takeuchi, K.; Nakao, A.; Katayama, C. *Acta Crystallogr., Sect. C: Cryst. Struct. Commun.* **1996**, *52*, 1008–1010. doi:10.1107/s0108270195013096
26. Cardullo, F.; Seiler, P.; Isaacs, L.; Nierengarten, J.-F.; Haldimann, R. F.; Diederich, F.; Mordasini-Denti, T.; Thiel, W.; Boudon, C.; Gisselhracht, J.-P.; Gross, M. *Helv. Chim. Acta* **1997**, *80*, 343–371. doi:10.1002/hlca.19970800203
27. Iversen, B. B.; Darovsky, A.; Bolotovskiy, R.; Coppens, P. *Acta Crystallogr., Sect. B: Struct. Sci.* **1998**, *54*, 174–179. doi:10.1107/s0108768197012007
28. Rispens, M. T.; Meetsma, A.; Rittberger, R.; Brabec, C. J.; Sariciftci, N. S.; Hummelen, J. C. *Chem. Commun.* **2003**, 2116–2118. doi:10.1039/b305988j
29. Nikawa, H.; Nakahodo, T.; Tsuchiya, T.; Wakahara, T.; Rahman, G. M. A.; Akasaka, T.; Maeda, Y.; Liu, M. T. H.; Meguro, A.; Kyushin, S.; Matsumoto, H.; Mizorogi, N.; Nagase, S. *Angew. Chem., Int. Ed.* **2005**, *44*, 7567–7570. doi:10.1002/anie.200502971
30. Ishitsuka, M. O.; Enoki, H.; Nikawa, H.; Wakahara, T.; Tsuchiya, T.; Akasaka, T.; Liu, M. T. H. *Tetrahedron Lett.* **2007**, *48*, 859–861. doi:10.1016/j.tetlet.2006.11.145
31. Sato, S.; Yamada, M.; Wakahara, T.; Tsuchiya, T.; Ishitsuka, M. O.; Akasaka, T.; Liu, M. T. H. *Tetrahedron Lett.* **2007**, *48*, 6290–6293. doi:10.1016/j.tetlet.2007.07.027
32. Matsuo, Y.; Okada, H.; Maruyama, M.; Sato, H.; Tobita, H.; Ono, Y.; Omote, K.; Kawachi, K.; Kasama, Y. *Org. Lett.* **2012**, *14*, 3784–3787. doi:10.1021/ol301671n
33. Okada, H.; Kawakami, H.; Aoyagi, S.; Matsuo, Y. *J. Org. Chem.* **2017**, *82*, 5868–5872. doi:10.1021/acs.joc.7b00730
34. Delker, G. L.; Wang, Y.; Stucky, G. D.; Lambert, R. L., Jr.; Haas, C. K.; Seyferth, D. J. *Am. Chem. Soc.* **1976**, *98*, 1779–1784. doi:10.1021/ja00423a024
35. Ando, W.; Fujita, M.; Yoshida, H.; Sekiguchi, A. *J. Am. Chem. Soc.* **1988**, *110*, 3310–3311. doi:10.1021/ja00218a056
36. Suzuki, H.; Tokitoh, N.; Okazaki, R. *J. Am. Chem. Soc.* **1994**, *116*, 11572–11573. doi:10.1021/ja00104a049
37. Suzuki, H.; Tokitoh, N.; Okazaki, R. *Bull. Chem. Soc. Jpn.* **1995**, *68*, 2471–2481. doi:10.1246/bcsj.68.2471
38. Ando, W.; Shiba, T.; Hidaka, T.; Morihashi, K.; Kikuchi, O. *J. Am. Chem. Soc.* **1997**, *119*, 3629–3630. doi:10.1021/ja9637412
39. Klapötke, T. M.; Kumar Vasisht, S.; Mayer, P. Z. *Anorg. Allg. Chem.* **2009**, *635*, 2447–2454. doi:10.1002/zaac.200900309
40. Ishida, S.; Iwamoto, T.; Kira, M. *Heteroat. Chem.* **2011**, *22*, 432–437. doi:10.1002/hc.20705
41. Pichaandi, K. R.; Mague, J. T.; Fink, M. J. *J. Organomet. Chem.* **2011**, *696*, 1957–1963. doi:10.1016/j.jorganchem.2010.10.043
42. Lips, F.; Fettinger, J. C.; Mansikkamäki, A.; Tuononen, H. M.; Power, P. P. *J. Am. Chem. Soc.* **2014**, *136*, 634–637. doi:10.1021/ja411951y
43. Ishikawa, M.; Matsuzawa, S.; Sugisawa, H.; Yano, F.; Kamitori, S.; Higuchi, T. *J. Am. Chem. Soc.* **1985**, *107*, 7706–7710. doi:10.1021/ja00311a080
44. Sato, K.; Kako, M.; Suzuki, M.; Mizorogi, N.; Tsuchiya, T.; Olmstead, M. M.; Balch, A. L.; Akasaka, T.; Nagase, S. *J. Am. Chem. Soc.* **2012**, *134*, 16033–16039. doi:10.1021/ja3073929
45. Becke, A. D. *Phys. Rev. A* **1988**, *38*, 3098–3100. doi:10.1103/physreva.38.3098
46. Becke, A. D. *J. Chem. Phys.* **1993**, *98*, 5648–5652. doi:10.1063/1.464913
47. Lee, C.; Yang, W.; Parr, R. G. *Phys. Rev. B* **1988**, *37*, 785–789. doi:10.1103/physrevb.37.785
48. Hehre, W. J.; Ditchfield, R.; Pople, J. A. *J. Chem. Phys.* **1972**, *56*, 2257–2261. doi:10.1063/1.1677527
49. Haddon, R. C. *J. Am. Chem. Soc.* **1997**, *119*, 1797–1798. doi:10.1021/ja9637659
50. Gaspar, P. P.; West, R. Silylenes. In *The Chemistry of Organosilicon Compounds*; Patai, S.; Rappoport, Z., Eds.; John Wiley & Sons: Chichester, UK, 1998; Vol. 2, pp 2463–2568. doi:10.1002/0470857250.ch43
51. Mizuhata, Y.; Sasamori, T.; Tokitoh, N. *Chem. Rev.* **2009**, *109*, 3479–3511. doi:10.1021/cr900093s
52. Suzuki, T.; Maruyama, Y.; Akasaka, T.; Ando, W.; Kobayashi, K.; Nagase, S. *J. Am. Chem. Soc.* **1994**, *116*, 1359–1363. doi:10.1021/ja00083a022
53. Akasaka, T.; Suzuki, T.; Maeda, Y.; Ara, M.; Wakahara, T.; Kobayashi, K.; Nagase, S.; Kako, M.; Nakadaira, Y.; Fujitsuka, M.; Ito, O. *J. Org. Chem.* **1999**, *64*, 566–569. doi:10.1021/jo981689h
54. Wakahara, T.; Han, A.; Niino, Y.; Maeda, Y.; Akasaka, T.; Suzuki, T.; Yamamoto, K.; Kako, M.; Nakadaira, Y.; Kobayashi, K.; Nagase, S. *J. Mater. Chem.* **2002**, *12*, 2061–2064. doi:10.1039/b201118b
55. Maeda, Y.; Aminur Rahman, G. M.; Wakahara, T.; Kako, M.; Okamura, M.; Sato, S.; Akasaka, T.; Kobayashi, K.; Nagase, S. *J. Org. Chem.* **2003**, *68*, 6791–6794. doi:10.1021/jo0344788
56. Han, A. H.; Wakahara, T.; Maeda, Y.; Akasaka, T.; Fujitsuka, M.; Ito, O.; Yamamoto, K.; Kako, M.; Kobayashi, K.; Nagase, S. *New J. Chem.* **2009**, *33*, 497–500. doi:10.1039/b808119k
57. Bourhis, L. J.; Dolomanov, O. V.; Gildea, R. J.; Howard, J. A. K.; Puschmann, H. *Acta Crystallogr., Sect. A: Found. Adv.* **2015**, *71*, 59–75. doi:10.1107/s2053273314022207
58. Sheldrick, G. M. *Acta Crystallogr., Sect. C: Struct. Chem.* **2015**, *71*, 3–8. doi:10.1107/s2053229614024218
59. Dolomanov, O. V.; Bourhis, L. J.; Gildea, R. J.; Howard, J. A. K.; Puschmann, H. *J. Appl. Crystallogr.* **2009**, *42*, 339–341. doi:10.1107/s0021889808042726
60. *Gaussian 16*, Revision C.01; Gaussian, Inc.: Wallingford, CT, 2019.

License and Terms

This is an open access article licensed under the terms of the Beilstein-Institut Open Access License Agreement (<https://www.beilstein-journals.org/bjoc/terms>), which is identical to the Creative Commons Attribution 4.0 International License (<https://creativecommons.org/licenses/by/4.0>). The reuse of material under this license requires that the author(s), source and license are credited. Third-party material in this article could be subject to other licenses (typically indicated in the credit line), and in this case, users are required to obtain permission from the license holder to reuse the material.

The definitive version of this article is the electronic one which can be found at:

<https://doi.org/10.3762/bjoc.20.100>